Aggregate Effects on the Thermal Shock Resistance of Spinel-Forming Refractory Castables

M.A.L. Braulio, G.B. Cintra, Y.W. Li, V.C. Pandolfelli

The performance of spinel forming refractory castables is mainly related to their slag corrosion and thermal shock behaviors. Concerning the thermal shock resistance, the aggregate selection is an important issue, as it can reduce the crack propagation and refractory damage. Therefore, this work addresses the effect of different aggregate sources (tabular alumina, electro-fused or sintered pre-formed spinels and electro-fused magnesia) in calcium aluminate cement (CAC)-bonded refractory castables. The calcium hexaluminate (CA_6) formation and its distribution throughout the castable microstructure played an outstanding role in the thermal shock resistance, pointing out the need for an appropriate microstructural design in order to attain a suitable performance during the castable application.

1 Introduction

Spinel-containing ($MgAl_2O_4$) refractory castables are widely used in the secondary steel-making processing equipment, mainly due to their outstanding basic slag resistance [1–4]. Besides corrosion, this class of castables should be able to withstand thermal cycling, retaining its mechanical integrity and inhibiting crack propagation which would increase the slag penetration. Considering these aspects, thermal shock resistance is an important issue when designing spinel-forming castables.

M.A.L. Braulio, G.B. Cintra, V.C. Pandolfelli
Federal University of São Carlos
Materials Engineering Department
Materials Microstructural Engineering Group
13565-905 São Carlos, SP
Brazil
(FIRE Associate Laboratory)

Y.W. Li
College of Materials & Metallurgy
Wuhan University of Science and Technology
430081 Wuhan
China

Corresponding author: *V.C. Pandolfelli*
E-Mail: vicpando@ufscar.com.br

Keywords: thermal shock resistance, calcium hexaluminate (CA_6), spinel-forming castables

Received: 30.05.2010
Revised 20.07.2010
Accepted: 22.07.2010

In order to initiate the crack propagation, the thermal stresses must be higher than the refractory mechanical strength, which is easily attained for thermal shocks in the range of 600 °C to 1200 °C. Thus, the most suitable alternative would be to minimize the damage [5, 6].

Besides selecting materials with lower thermal expansion coefficient (α), high thermal conductivity and diffusivity, as well as lower elastic modulus (E), in order to increase the thermal shock resistance, other suitable ways of increasing the refractory crack propagation resistance should be analyzed. Among them, the aggregate selection, the design of the pore size distribution, the liquid phase viscosity based on the purity and selection of raw materials, the microcracking network and the presence of needle-like shaped phases are practical options which deserve further studies.

Concerning the aggregates, they can inhibit the crack propagation via two routes: by crack deflection and as a barrier, if the crack is trans-granular.

The micro-crack network also leads to further energy dissipation [7]. The higher their amount, the higher the refractory fracture energy would be. Nevertheless, micro-cracking, depending on its amount per volume, results in crack coalescence, reducing its overall content but increasing its size. This could result in further drawbacks, such as lower slag infiltration resistance and lower mechanical strength. In spinel-forming refractory castables, micro-cracks can be generated by in-situ formation of expansive phases ($MgAl_2O_4$ and CA_6) [8–10] or due to differential thermal expansions during heating or cooling [11–13].

Refractory toughening can also be induced by the presence of high aspect ratio phases. For calcium aluminate cement-bonded spinel-containing castables, this can be attained by the in-situ formation of calcium hexaluminate (CA_6), which, for liquid containing systems, results in acicular morphologies [14, 15]. According to *Fuhrer* et al. [16], the interlocked CA_6 plates or needles would provide good thermal shock resistance, due to toughening mechanisms such as crack bridging and deflection. The interlocked CA_6-matrix-aggregate microstructure also induces higher castable hot modulus of rupture and creep resistance [17].

Considering that the thermal shock damage understanding of spinel-forming refractory castables is essential for a suitable performance in steel ladle working conditions and that *Sarpoolaky* and colleagues [18] have already highlighted the effects of larger grains on the slag corrosion of low-cement containing castables, this work addressed the performance of various aggregate sources (tabular alumina, pre-formed spinel or electro-fused magnesia) for spinel-forming and CAC-containing castables regarding their thermal shock resistance.

Additional tests were carried out (permanent linear expansion, SEM and XRD quantitative analyses, thermal expansion coefficient measurements) in order to provide microstructural information and support to the thermal shock attained results.

2 Materials and techniques

Vibratable castable compositions were designed according to the Alfred particle packing model (q = 0,26) [19]. The castables' matrix comprised 6 mass-% of dead-burnt magnesia (< 45 µm, 95 mass-% of MgO, CaO/SiO_2 ratio = 0,37, *Magnesita Refratários* S.A., Brazil), 1 mass-% of microsilica (971U, *Elkem*, Norway) and 7 mass-% of reactive alumina (CL370, *Almatis*, USA). Tabular alumina (d ≤ 6 mm, *Almatis*, Germany), sintered spinel (d ≤ 6 mm, 90 mass-% Al_2O_3 and 10 mass-% MgO *Almatis*, Germany), electro-fused spinel (d ≤ 4,75 mm, 76 mass-% Al_2O_3 – 24 mass-% MgO, *Magnesita Refratários S.A.*, Brazil) and electro-fused magnesia (d ≤ 4,75 mm, 97 mass-% MgO, CaO/SiO_2 = 3,5, *Magnesita Refratários S.A.*, Brazil) were used as refractory aggregates. An electro-steric dispersing agent was added in order to ensure the matrix dispersion (*BASF*, Germany) and 4,1 mass-% of water provided a suitable molding under vibration. Tab. 1 shows the castable compositions.

After mixing, the castables were shaped (25 x 25 x 150 mm³) and following their processing (1 d curing at 50 °C in a humid environment, 1 d drying at 110 °C and prefiring at 600 °C for 5 h), they were fired at 1150, 1300 and 1500 °C for 5 h (heating rate = 1 °C/min) in order to evaluate the cold modulus of rupture (CMOR, 3-point-bending tests), the permanent linear expansion (PLE), the apparent porosity and the cycling thermal shock resistance.

The mechanical evaluation was conducted according to the ASTM C133-94 standard using MTS testing equipment (*MTS Systems*, Model 810, USA). SEM analyses were carried out using a JEOL JSM 5900 LV microscope, whereas phase evaluation (mainly CA_6) was attained by XRD quantitative analyses (TOPAS 4.1, *Bruker*, Germany). The apparent porosity of the fired samples was measured by the Archimedes technique in kerosene and the permanent linear expansion (PLE) was evaluated by the difference between the initial and final length of bar samples, before and after firing at 1150, 1300 and 1500 °C for 5 h.

Concerning the thermal shock test, the castables were subjected to several heating and cooling cycles. The samples were placed into a furnace chamber previously heated up to 1025 °C and kept at this temperature for 15 min. Afterwards, they were withdrawn from the furnace and cooled in air, leading to a thermal gradient of roughly 1000 °C. After

Tab. 1 Castable compositions evaluated in this work

	Compositions [mass-%]			
Raw materials	**TA**	**Sp90**	**Sp76**	**Mag**
Tabular alumina (d ≤ 6 mm)	62	0	0	0
Sintered spinel (alumina-rich, 90 mass-% Al_2O_3, d ≤ 6 mm)	0	62	0	0
Electro-fused spinel (alumina-rich, 76 mass-% Al_2O_3, d ≤ 4,75 mm)	0	0	62	0
Electro-fused magnesia (d ≤ 4,75 mm)	0	0	0	72
Reactive and tabular alumina (d ≤ 200 m)	25	25	25	15
Dead burnt magnesia (d ≤ 45 m)	6	6	6	6
Silica fume	1	1	1	1
Calcium aluminate cement	6	6	6	6

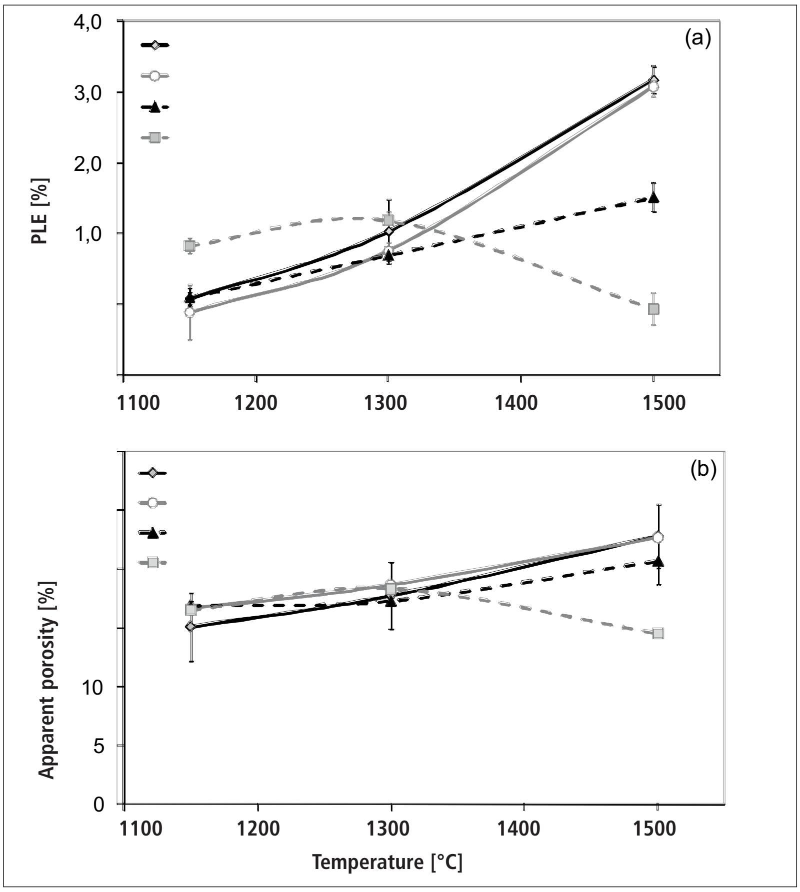

Fig. 1 a) Permanent linear expansion (PLE) and b) apparent porosity as a function of the firing temperature

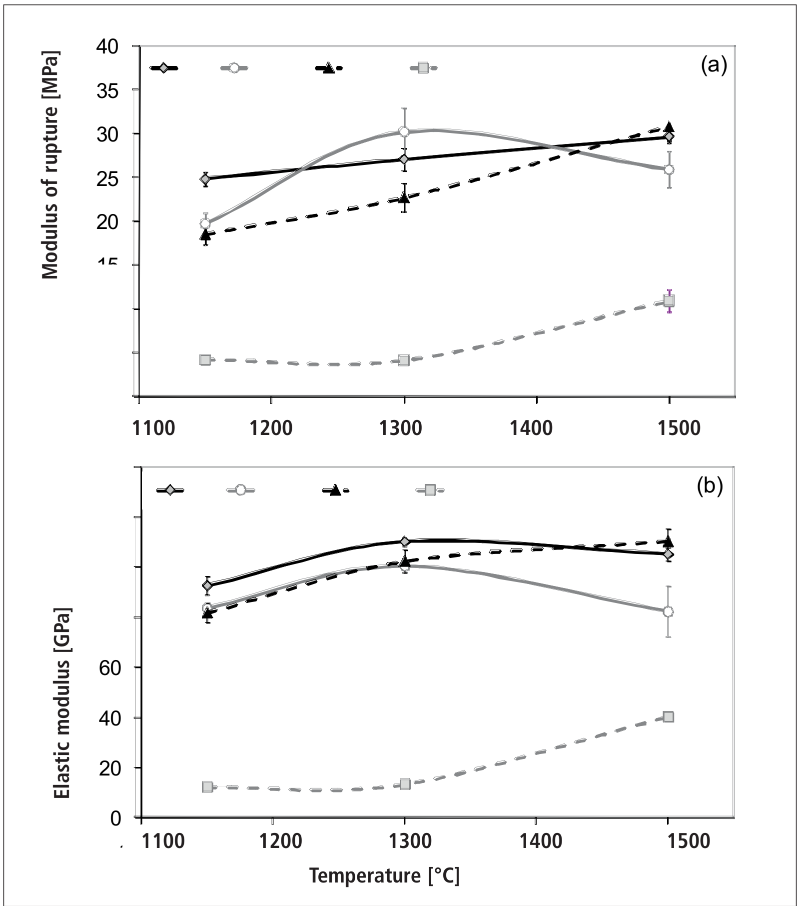

Fig. 2a Modulus of rupture and b) elastic modulus as a function of the firing temperature

Tab. 2 Modulus of rupture, before and after 10 thermal shock cycles

Thermal shock damage (for castables fired at 1500 °C)				
	TA	**Sp90**	**Sp76**	**Mag**
Mechanical strength [MPa]	29,7 ± 0,7	26,0 ± 2,1	30,9 ± 1,6	11,0 ± 1,3
Mechanical strength - after 10 thermal shock cycles [MPa]	5,7 ± 2,3	1,5 ± 0,3	0	0

15 min at room temperature, the cycling was repeated as required.

The thermal shock damage was evaluated by the elastic modulus measurements (bar resonance – ASTM C-1198 standard) as a function of the thermal cycles (0, 2, 4, 6, 8 or 10 cycles). Considering that a non-destructive test was used, the elastic modulus decay was followed in the same sample, as a function of the thermal shock cycling.

3 Results and discussion

Fig. 1 shows the permanent linear expansion (PLE) and apparent porosity results as a function of firing temperature (1150, 1300 or 1500 °C for 5 h), pointing out that the refractory aggregates affect the castable volumetric stability, as previously reported by the authors [11]. Both PLE and porosity slightly increased from 1150 to 1300 °C, due to the in-situ spinel formation [8–10], as all compositions comprised a similar matrix (6 mass-% of dead-burnt MgO and at least 15 mass-% of fine Al_2O_3).

However, from 1300 to 1500 °C, shrinkage was detected for the electro-fused MgO-containing castable (Mag), whereas the ones containing spinels (Sp76 or Sp90) or tabular alumina (TA) resulted in further expansion. The apparent porosity followed the PLE curve trends. In general, after firing at 1500 °C, the reduction of the aggregate alumina content led to lower linear expansion level (PLE ranking: Mag < Sp76 < Sp90 < TA), which is most likely a consequence of the calcium hexaluminate (CA_6) formation, as will be discussed later.

Concerning the mechanical and elastic properties, the use of electro-fused MgO aggregates resulted in lower values than the ones attained by adding spinels or tabular alumina as aggregates (Fig. 2). This can be related to the thermal expansion coefficient mismatch between the matrix compounds (Al_2O_3 / $MgAl_2O_4$, $\alpha \sim 8 \cdot 10^{-6}$ °C^{-1}) and the aggregates (MgO, $\alpha \sim 13 \cdot 10^{-6}$ °C^{-1}), leading to a greater amount of micro-cracks [12].

For the other compositions, a drop in the elastic modulus was detected for the TA and Sp90 compositions at 1500 °C, indicating the effect of the CA_6 formation and the associated micro-cracks, as the content of in-situ spinel was nearly the same for the four compositions (6 mass-% of dead-burnt MgO was added to their matrices and the spinel formation took place mainly in the 1150 – 1300 °C temperature range). Nevertheless, whereas the mechanical strength and elastic modulus behavior were in agreement for the Sp90 castable, the same did not happen for the TA composition. This aspect points out that the elastic modulus is more sensitive to the castable microstructural features. The lower PLE of the Sp76 castable (Fig. 1a), compared with the ones attained for the TA or Sp90 compositions, indicates lower micro-cracking level or coalescence and, therefore, the elastic modulus and the mechanical strength increased with the firing temperature, as the CA_6 content was the same for all compositions after firing at 1500 °C. This will be presented later.

After this initial analysis and aiming to evaluate the thermal shock damage after the development of the high temperature expansive phases (spinel and CA_6), the thermal shock resistance was measured (E value profile as a function of thermal cycling with ΔT = 1000 °C) for the samples fired at 1500 °C for 5 h (Fig. 3).

The spinel or electro-fused MgO-containing castables showed poor thermal shock resistance and, for Mag and Sp76 compositions, the samples fractured after four thermal cycles (Fig. 4). Although the composition Sp90 did not split apart during the test, its elastic modulus decay was higher than the one observed for the TA castable.

Tab. 2 shows the modulus of rupture values, before and after thermal shock (10 cycles), stressing the best performance for the tabular alumina (TA)-containing composition.

In order to understand the main reasons for such a different thermal shock behavior, XRD quantitative analyses and SEM evaluation were carried out.

Concerning the expansive phase generation, all castables presented roughly 21 mass-% of spinel and 15 – 16 mass-% of calcium hexaluminate (CA_6), after firing at 1500 °C for 5 h. Although the amount of CA_6 was nearly the same for all compositions, its distribution throughout the castable microstructures was distinct (Fig. 5). The tabular alumina (TA)-containing composition showed CA_6 grains mainly at the border of the aggregates (although a slight amount was also found inside of the grain), whereas this phase was only detected in the matrix for the Sp76 composition, pointing out no matrix-aggregate interlocking effect as the grain surfaces were clean (without any reaction). With an intermediate behavior, the Sp90 castable contained CA_6 in both regions: inside its aggregates, but also in the matrix. For the Mag castable, no CA_6 was detected, as previously shown by the authors [11].

Considering this aspect, the thermal shock behavior is strongly affected by the CA_6 distribution and the higher its formation inside and/or at the edge of the refractory aggregates, the better the thermal shock resistance, owing to higher matrix-aggregate interlocking.

A further aspect for the best thermal shock result attained for the TA castable is associated with the tabular alumina grain microstructure, which comprises a high amount of closed spherical pores.

This feature increases the thermal shock resistance by making the crack propagation more difficult, due to a tortuous crack path inside the grain and to the increase the radius of curvature of the crack tip when reaching a closed pore.

The electro-fused aggregates (present in the Sp76 or Mag compositions) are denser and, thus, more prone to catastrophic crack propagation.

For the MgO electro-fused aggregates, the low thermal shock resistance is also a consequence of its high thermal expansion coefficient (α), as shown in Tab. 3.

Taking these aspects into account and besides the aggregate microstructures and their thermal expansion coefficient effects, the alumina content in the aggregates is a key-issue for calcium aluminate cement-bonded castables, as it will define the

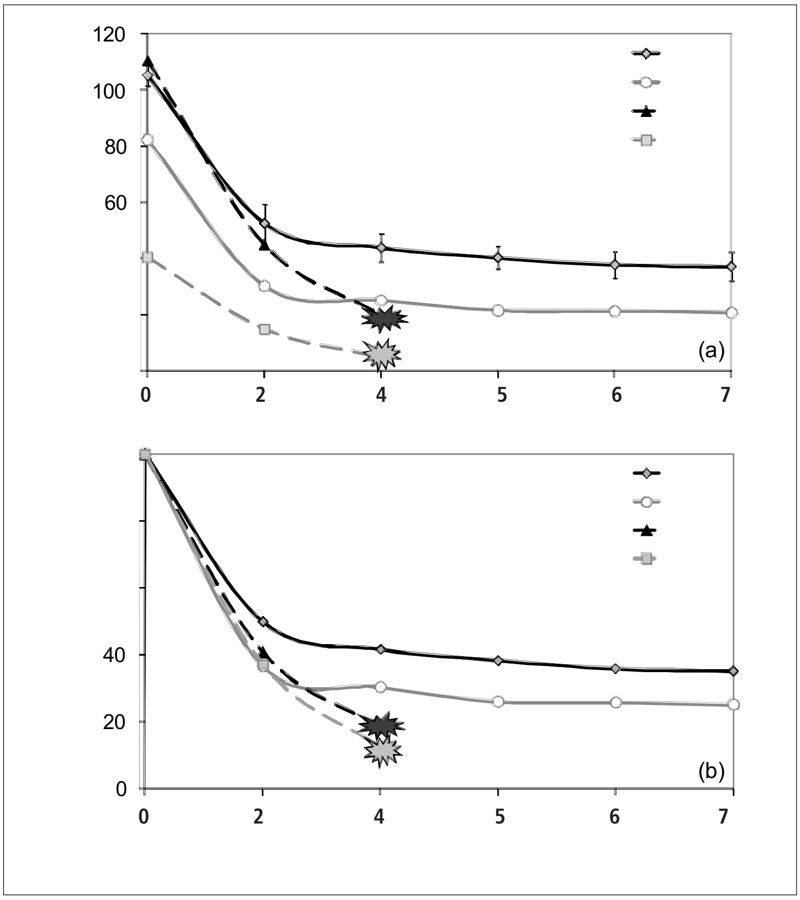

Fig. 3 Thermal shock evaluation (T = 1000 °C) as a function of the number of cycles, for castables previously fired at 1500 °C for 5 h, presented as a) E absolute values, and b) E normalized values

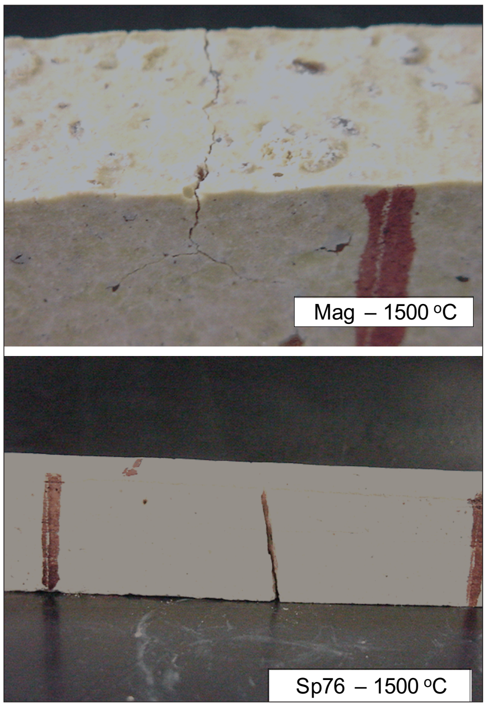

Fig. 4 Fractures detected during the thermal shock cycling for the compositons Mag and Sp76

Tab. 3 Thermal expansion coefficient (α)

Thermal expansion coefficient (for castables fired at 1500 °C)				
	TA	Sp90	Sp76	Mag
α [$10^{-6}\cdot{}^{\circ}C^{-1}$]	8,4	8,6	8,7	11,2

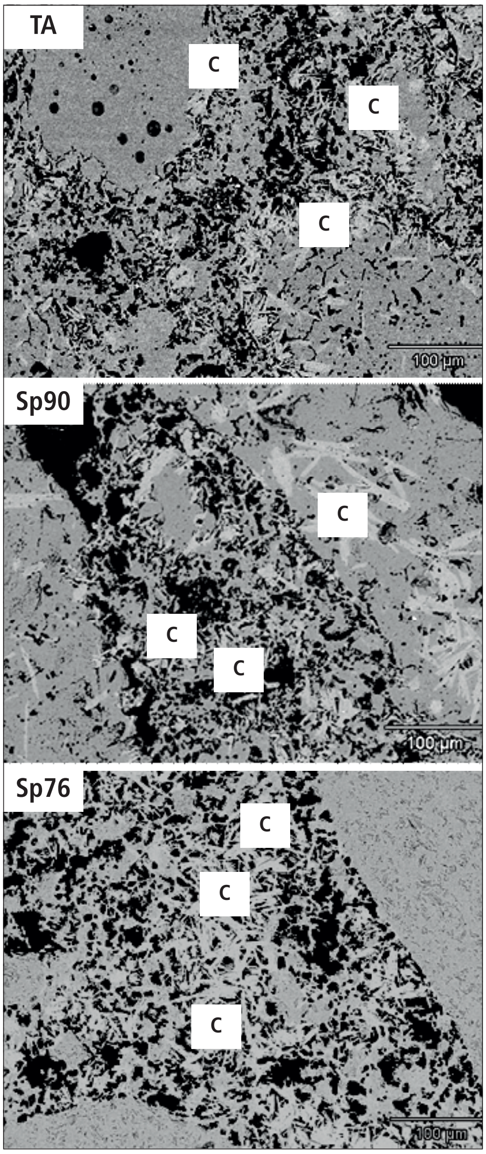

Fig. 5 Castable microstructures of the CA_6-containing (C) compositions (TA, Sp90 or Sp76), pointing out this phase distribution, after firing at 1500 °C for 5 h

castable CA_6 distribution and thus directly affect their thermal shock resistance.

5 Conclusions

Before the thermal shock tests, the thermally treated (1150, 1300 or 1500 °C) castables showed different expansion, porosity, cold modulus of rupture and elastic modulus levels, highlighting that the refractory aggregates are active partners during the castable sintering.

The main difference detected among the evaluated compositions was the CA_6 distribution in the castable microstructure, as this phase content was nearly the same for the alumina-containing aggregate castables.

Therefore, the thermal shock resistance was mainly affected by this feature and, the higher the bridging between the aggregates and the matrix, owing to the CA_6 grain formation at the grain edges, the better the thermal shock resistance of this sort of castables.

Acknowledgments

The authors are grateful to the *Federation for International Refractory Research and Education (FIRE)*, *Magnesita Refratários S.A.* (Brazil), *Corus - Ceramics Research Centre* (the Netherlands) and *Brazilian Research Funding Agency FAPESP* for supporting this work.

In addition, the authors are thankful to *D.H. Milanez* and *E.Y. Sako* for the castable processing.

References

[1] Nagasoe, A.: Tsurumoto, S.I.; Kitamura, A.: Refractory characteristics of spinels with various MgO contents. Taikabutsu Overseas. 11 (1991) [3] 20–28

[2] Mori, J.; Yoshimura, M.; Oguchi, Y.; Kawakami, T.; Ohishi, I.: Effect of slag composition on wear of alumina-spinel castable for steel ladle. Taikabutsu Overseas. 12 (1992) [1] 40–45

[3] Naigai, B.; Matsumoto, O.; Isobe, T.; Nishiumi, Y.: Wear mechanism of castable for steel ladle by slag. Taikabutsu Overseas 12 (1992) [1] 15–20

[4] Bartha, P.; Markworth, M.; Schadock, J.; Södje, J.; Diesing, H.: Contribution to melt refinement of special steels with calcium aluminate in open induction furnaces. refractories WORLDFORUM 2 (2010) [1] 72–80

[5] Pandolfelli, V.C.: Thermal shock resistance of engineered microstructure. Short course UNITECR 2009, Salvador, Brazil, 2009

[6] Homeny, J.; Bradt, R.C.: Thermal shock of refractories – thermal stress in materials and structures in severe thermal environments. (1980) pp. 343–363

[7] Faber, K.T.: Toughening mechanisms for ceramics in automotive applications. Ceram. Engng. Sci. 5 (1984) 408–436

[8] Ko, Y.C., Lay, J.T.: Thermal expansion characteristics of alumina-magnesia and alumina-spinel castables in the temperature range 800 – 1650 °C. J. Am. Ceram. Soc. 83 (2000) [11] 2872–2874

[9] Ide, K.; Suzuki, T.; Asano, K.; Nishi, T.; Ichikawa, H.: Expansion behavior of alumina-magnesia castables. J. Techn. Ass. Refr. Japan. 25 (2005) [3] 202–208

[10] Braulio, M.A.L.; Milanez, D.H.; Sako, E.Y.; Bittencourt, L.R.M.; Pandolfelli, V.C.: Expansion behavior of cement-bonded alumina-magnesia refractory castables. Am. Ceram. Soc. Bull. 86 (2007) [12] 9201–9206

[11] Braulio, M.A.L.; Milanez, D.H.; Sako, E.Y.; Bittencourt, L.R.M.; Pandolfelli, V.C.: Are refractory aggregates inert?. Am. Ceram. Soc. Bull.87 (2007) [3] 27–31

[12] Rigaud, M.; Palco, S.; Wang, N.: Spinel formation in the MgO–$MgAl_2O_4$ system relevant to basic castables. In: Proc. UNITECR (1995) 387–394

[13] Braulio, M.A.L.; Bittencourt, L.R.M.; Pandolfelli, V.C.: Magnesia grain size effect on in-situ spinel refractory castables. J. Eur. Ceram. Soc. 28 (2008) 2845–2852

[14] An, L.; Chan, H.M.; Soni, K.K.: Control of calcium hexaluminate grain morphology in in-situ toughened ceramic composites. J. Mat. Sci. 31 (1996) 3223–3229

[15] Braulio, M.A.L.; Bittencourt, L.R.M.; Poirier, J.; Pandolfelli, V.C.: Microsilica effects on cement-bonded alumina–magnesia refractory castables. J. Techn. Ass. Refr. Japan 28 (2008) [3] 180–184

[16] Fuhrer, M.; Hey, A.; Lee, W.E.: Microstructural evolution in self-forming spinel/calcium aluminate-bonded castable refractories. J. Eur. Ceram. Soc. 18 (1998) 813 – 820

[17] Ko, Y.C.; Chan, C.F.: Effect of spinel content on hot strength of alumina-spinel castables in the temperature range 1000–1500 °C. J. Eur. Ceram. Soc. 19 (1999) 2633–2639

[18] Sarpoolaky, H.; Zhang, S.; Lee, W.E.: Corrosion of high alumina and near stoichiometric spinels in iron-containing silicate slags. J. Eur. Ceram. Soc. 23 (2003) 293–300

[19] Funk, J.E.; Dinger, D.R.: Particle packing, Part III: Discrete versus continuous particle sizes. Interceram 41 (1992) [5] 332–333